Influence of the depletion length on the commensurability effects in tunable antidots

T. Deruelle
Laboratoire de Physique de la Matière Condensée, Ecole Normale Supérieure, 24 rue Lhomond, F-75231 Paris Cedex 05, France

B. Meurer
Laboratoire de Physique de la Matière Condensée, Ecole Normale Supérieure, 24 rue Lhomond, F-75231 Paris Cedex 05, France
and Max-Planck-Institut für Festkörperforschung, Heisenbergstraße 1, D-70569 Stuttgart, Germany

Y. Guldner and J. P. Vieren
Laboratoire de Physique de la Matière Condensée, Ecole Normale Supérieure, 24 rue Lhomond, F-75231 Paris Cedex 05, France

M. Riek, D. Weiss, K. von Klitzing, and K. Eberl
Max-Planck-Institut für Festkörperforschung, Heisenbergstraße 1, D-70569 Stuttgart, Germany

K. Ploog
Paul-Drude-Institut für Festkörperelektronik, Hausvogteiplatz 5-7, D-10117 Berlin, Germany
(Received 17 February 1994)

Commensurability effects between the period of an artificial array of scatterers (antidots) in a two-dimensional electron gas and the classical cyclotron radius are found to depend strongly on the size of the antidots in comparison with the period. Magnetotransport experiments on tunable antidot arrays are reported and analyzed. In the region of large depletion zones we find strong deviations of the Hall effect from the Drude slope in magnetic fields up to several teslas. From this, we deduce undepleted regions of less than 60 nm in typical 500-nm period structures. The suppression of the commensurability motion around several antidots observed in the longitudinal magnetoresistance in the case of strong depletion has the same origin and allows us to determine independently and consistently the depletion radius of the antidots.

Low-dimensional quantum confined electronic systems in semiconductors have recently attracted much interest. The ultimate limit is a quantum dot, where few electrons are confined in all three dimensions.[1–7] The reverse structures with respect to dots are antidots, i.e., periodic scattering centers in a high-mobility two-dimensional electron gas (2DEG). In these structures commensurability effects between the periodic structure and the cyclotron radius in a magnetic field have been observed.[8–15]

We present magnetotransport experiments on field-effect-confined antidot lattices where we can widely tune the size of the depletion length of the antidots via a gate voltage. Thus detailed studies of the depletion effects are possible. In particular, we can define a situation where the sizes of the antidots are much larger than half the period of the microstructure. The electron mobility remains high in the undepleted regions between the antidots, yielding well developed quantum Hall plateaus in moderate magnetic fields. We observe a strong dependence of the commensurability effects on the depletion, which is adjusted by the gate voltage. At high gate voltages (strong depletion), the commensurability peak corresponding to the electron motion around four antidots vanishes. In this situation we find drastic deviations of the Hall resistance from the expected behavior over a wide magnetic field range from zero to about 2 T for structures of 500 nm period. In particular, the deviations include part of the quantized region. The results are analyzed in the framework of a billiard model that allows one to determine the depletion radius of the antidots as a function of V_g, which is consistent with the features observed in both the magnetoresistance and the Hall resistance.

The antidot structures have been prepared at the Max-Planck-Institut in Stuttgart starting from $Al_{0.32}Ga_{0.68}As$-GaAs heterostructures grown by molecular beam epitaxy. The thicknesses of the spacer layer, of the doped $Al_xGa_{1-x}As$ layer, and of the cap layer are 26, 45, and 11 nm, respectively. By wet chemical etching, we have defined 100 μm wide Hall bar structures with a contact separation of 180 μm. Ohmic contacts to the 2DEG are created by alloying AuGe-Ni at 450 °C for 1 min. On top of the Hall bars, we prepared a periodic photoresist antidot array in the photoresist by holographic lithography with periods a down to 400 nm. A 5 nm thick semitransparent NiCr gate was evaporated onto the photoresist structure. The patterned samples have 2D electron densities $N_s = 2 \times 10^{11}$ cm^{-2} and mobilities $\mu \approx 200\,000$

$cm^2/V\,s$ (at 1.7 K). With a gate voltage, we can vary N_s and the strength of the periodic potential modulation acting on the electron gas. At high negative gate voltages V_g, regions where the gate is closer to the electron channel are depleted, resulting in an antidot lattice in the electron gas. By further increasing V_g, the structure becomes more and more depleted, leading to "holes" in the electron sea which can be much larger than the geometrical size of the photoresist mask. In this limit, we have quantum dots connected by narrow constrictions. Magnetotransport experiments at $T = 1.7$ K in perpendicular magnetic fields B are performed with standard lock-in technique at 13.3 Hz frequency using currents of 0.5 μA. The electron density can be raised to $N_s = 4$–5×10^{11} cm^{-2} with a mobility $\mu = 500\,000$ $cm^2/V\,s$ (at 1.7 K) by briefly illuminating with a red light-emitting diode (LED). Thus we can study systems with several electron densities. We present hereafter results on two samples, labeled 1 and 2 with periods $a = 500$ nm and $a = 1$ μm, respectively.

Figure 1(a) shows the longitudinal magnetoresistance ρ_{xx} obtained for sample 1 illuminated at three different gate voltages in the antidot regime. The inset presents the magnetoresistance up to $B = 12$ T for a gate voltage $V_g = -1.8$ V. Note that, even in this situation of strong depletion, the resistance drops to zero at even filling factors and the spin splitting of the Shubnikov–de Haas oscillations as well as signatures of the fractional quantum Hall effect around $\nu = 4/3$ are well observed, demonstrating the high quality of these antidot structures. The electron mobility at $V_g = 0$, as deduced from ρ_{xx} at $B = 0$, is $\mu = 480\,000$ $cm^2/V\,s$ with $N_s = 4\times10^{11}$ cm^{-2}, from which we calculate an elastic mean free path $l_0 = \frac{\hbar}{e}\sqrt{2\pi N_s}\mu \approx 5$ μm, much larger than the period of the antidot lattice.

Several pieces of information can be obtained from the analysis of the magnetoresistance ρ_{xx} as a function of the magnetic field. In the gate voltage range from 0 to -2 V, Shubnikov–de Haas oscillations indicate that N_s decreases from 4×10^{11} cm^{-2} at $V_g = 0$ to 3.2×10^{11} cm^{-2} at $V_g = -2$ V. At low magnetic fields, two prominent commensurability peaks, labeled 1 and 4 in Fig. 1(a), are observed. Peak 1 clearly reflects the commensurability of the classical cyclotron radius $r_c = \frac{\hbar}{eB}\sqrt{2\pi N_s}$ with the periodicity a of the structure when $r_c = \frac{a}{2}$. This is confirmed for all measured samples with periods from 1 μm to 400 nm and for all carrier densities. For example, in Fig. 1, this peak at $V_g = -1.2$ V occurs at $B = 0.4$ T with $N_s = 3.6\times10^{11}$ cm^{-2} leading to $r_c = 248$ nm, which is exactly half the period of the structure. Peak 4 occurring at $B \approx 0.15$ T, which corresponds to $r_c = 660$ nm, is related to a collision-free motion of an electron around four antidots. Taking into account the mean free path in between the antidots of about $l_0 = 4.8$ μm, this motion is still observable unlike even longer orbits around 9 or 21 antidots.[8,16]

Even though the microscopic potential profile may be complicated, a simple billiard model can lead to a fairly good estimation of the occurrence of peak 4 as sketched in Fig. 1(b) for two different gate voltages $V_{g1} \le V_{g2}$. Indeed, within such a model, motions around four antidots are permitted as long as the depletion radius r_d is sufficiently small, e.g., as long as the condition $\frac{a}{\sqrt{2}} + r_d \le r_c \le \frac{a}{\sqrt{2}}\sqrt{5} - r_d$ is fulfilled [the two extreme orbits are shown in Fig. 1(b) for V_{g1}]. Taking into account the average radius $r_c = \frac{a}{2}(\sqrt{\frac{5}{2}} + \sqrt{\frac{1}{2}})$ leads to $B = 0.17$ T for peak 4, in good agreement with the experiments. Quite similar results are observed in all the samples we have studied. Furthermore, as the gate voltage is increased, the commensurability peak 4 vanishes around -1.8 V (Fig. 1). Two phenomena can account for this suppression: the change in the potential profile[16] and also the enlargement of the depletion radius, as sketched in Fig. 1(b) for V_{g2}. It has been shown elsewhere[17] that the

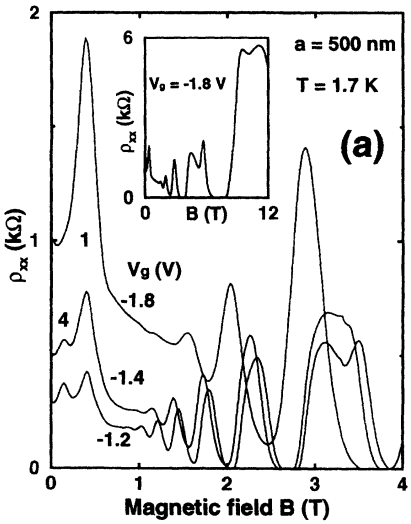

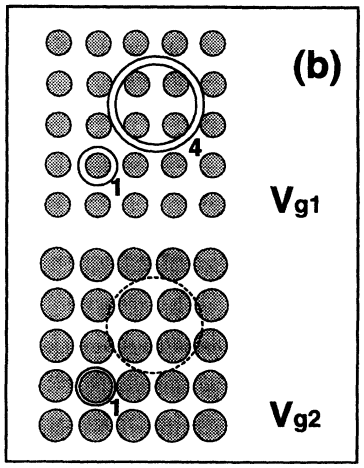

FIG. 1. (a) Magnetoresistance ρ_{xx} for sample 1 with a period of $a = 500$ nm at three different gate voltages V_g as indicated. Commensurability peaks around one and four antidots (labeled 1 and 4) are observed. Peak 4 vanishes at large voltages (large depletion). The inset shows the high-field data at $V_g = -1.8$ V. The temperature is $T = 1.7$ K. (b) Schematic billiard model for different sizes of the depletion zone ($-V_{g2} \ge -V_{g1}$). For strong depletion the motion around four antidots is no longer possible.

depletion radius increases drastically if the average electron density within the unit cell decreases. Moreover, it has been demonstrated recently[18] that the electronic density measured by magnetotransport in antidot arrays represents the density in between the antidots and not the average density over a cell. Therefore, the mean free path in between the antidots is always very long since it depends on the carrier density N_s which is changed only by 20% from $V_g = 0$ to $V_g = -1.8$ V. As a consequence, the commensurability peak does not disappear because of a reduction of the intrinsic mobility. Peak 1 becomes even more pronounced at high gate voltages and reaches as much as 100% of the zero-field resistance [see Fig. 1(a)]. In fact, as V_g increases, the depletion radius r_d is enhanced and the range of magnetic fields where the motion around four antidots is possible decreases. In the limit where $\frac{a}{\sqrt{2}} + r_d = \frac{a}{\sqrt{2}}\sqrt{5} - r_d$, e.g., $r_d = \frac{a}{2}(\sqrt{\frac{5}{2}} - \sqrt{\frac{1}{2}})$, no orbit around four antidots can exist anymore [the two extreme orbits labeled 4 in Fig. 1(b) merge into one another]. We get thus a first estimation of the critical depletion radius $r_d^{\text{crit}} = 218$ nm, close to the maximum possible value of 250 nm (connected quantum dots). Therefore the width of the constriction between two antidots is only ≈ 64 nm in this configuration. This small value has drastic consequences on the transverse magnetoresistances ρ_{xy}. Figure 2 shows ρ_{xy} for sample 1 at several gate voltages. As V_g increases, the Hall effect strongly deviates from the Drude slope (dashed lines) at small magnetic fields. At $V_g = -1.2$ V, this deviation is observed until ≈ 1.2 T and until ≈ 2 T at $V_g = -1.8$ V.

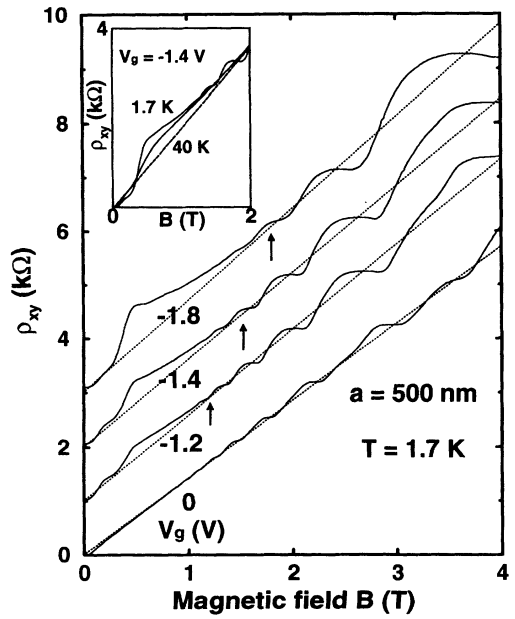

FIG. 2. Hall resistance ρ_{xy} for sample 1. Deviations of the Hall resistance from the classical Drude slope (dashed lines) are observed that depend largely on the depletion radius. In the case of high depletion ($V_g = -1.8$ V), deviations up to a magnetic field of 2 T are found. The onsets of the deviations are marked with arrows. The inset shows the Hall effect at 1.7 K and 40 K for a gate voltage $V_g = -1.4$ V.

This effect is purely classical, contrary to the plateaus of the quantum Hall effect which also begin to develop in this region. Indeed it persists when the temperature is increased. At 40 K, a significant deviation from the Drude line still remains whereas the Hall plateaus have disappeared much below this temperature (see inset of Fig. 2). Such deviations were predicted[19] for narrow channel 2DEG's, which corresponds to the situation of our sample at high gate voltages. Beenakker and van Houten[19] showed that the onset of deviations occurs for magnetic fields beyond which a cyclotron orbit can no longer intersect the channel walls between two antidots (see inset of Fig. 3). The critical magnetic fields, indicated by arrows in Fig. 2, correspond to the condition $r_c = \frac{a}{2} - r_d$. From this analysis, we find in particular for $V_g = -1.8$ V a depletion radius $r_d = 203$ nm, in very good agreement with the value of 218 nm obtained for the disappearance of peak 4. This strongly supports the idea that both effects are caused by the large depletion radius. Note that the motion around four antidots and therefore its suppression were not observed in the previous work on tunable antidot arrays,[11] demonstrating the high quality of our structures.

Results obtained for sample 2 with a period $a = 1$ μm confirm this analysis. In Fig. 3 the magnetoresistance and the Hall resistance for sample 2 are plotted for a gate voltage $V_g = -3$ V. Commensurability effects around one and four antidots are clearly resolved. (Note that with nearly the same N_s as for sample 1, the commensurability features appear at half the value of the magnetic field because the period is twice as large.) For $V_g = -3$ V and $N_s = 3.3 \times 10^{11}$ cm^{-2}, peak 1 occurs at $B = 0.19$ T, corresponding to a classical cyclotron radius $r_c = 480$ nm, which is practically half the period of the structure.

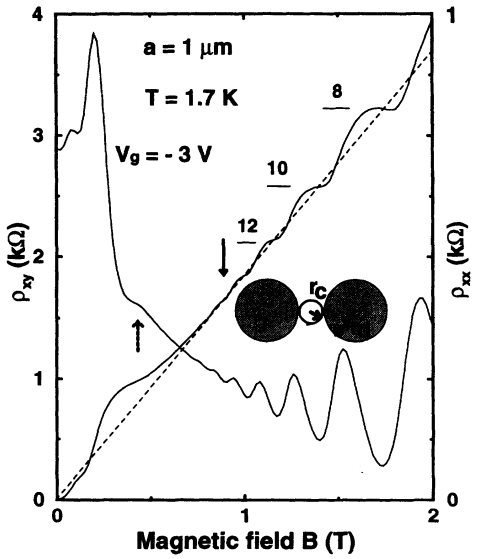

FIG. 3. Magnetoresistance and Hall resistance for sample 2 with a period $a = 1$ μm at $V_g = -3$ V. The solid arrow marks the onset of the observed deviation from which the radius of depletion r_d can be calculated (see inset and text). Weaker structures (marked by a dashed arrow) are associated with interference effects in the potential landscape of the antidots.

Peak 4 is found at $B = 0.08$ T, giving $r_c = 1250$ nm which is, as expected, twice as large as for sample 1. Our model predicts a value of 0.09 T for peak 4. The onset of the deviation of the Hall effect at ≈ 0.9 T gives $r_d \approx 400$ nm, which is close to the critical value of 437 nm predicted by our model for the vanishing of peak 4. Indeed peak 4 is experimentally found to disappear at $V_g = -3.5$ V.

In all samples we observe additional structures on the classical Hall plateau (Fig. 2) and in the magnetoresistance (dashed arrow in Fig. 3). Concerning the classical Hall plateau these extra structures were explained theoretically for ballistic microjunctions[19,20] and very recently for antidot arrays[21] in terms of interference effects, depending on the actual potential form of the antidots.

In summary, we have presented magnetotransport studies on widely tunable antidot lattices. We could study the influence of the antidot depletion length on the commensurability effects. We were able to realize a situation of strong depletion, e.g., large antidots in comparison with the period, in which drastic magnetoresistance peaks and deviations of the Hall effect in magnetic fields up to several teslas are observed. In a billiard model, we could consistently determine the depletion radius r_d from the suppression of the commensurability peak around four antidots and from the deviations of the Hall curve. We have thus determined the dependence of r_d as a function of the gate voltage. Small oscillations on the Hall plateaus and in the magnetoresistance show details of the confining potential.

We wish to acknowledge most useful discussions with Elisabeth Vasiliadou, Daniela Pfannkuche, M. Voos, G. Bastard, and D. Heitmann. We thank R. Nötzel, A. Fischer, and M. Hauser for the molecular beam epitaxy growth of our samples, and C. Lange for expert help with the preparation of the dots. We acknowledge financial support from the Bundesministerium für Forschung und Technologie and from the European Community. The Laboratoire de Physique de la Matiere Condensée de l'Ecole Normale Superieure Unité associée au Centre Nationale de la Recherche Scientifique, and is associated with University Paris 6.

[1] Ch. Sikorski and U. Merkt, Phys. Rev. Lett. **62**, 2164 (1989).
[2] W. Hansen, T. P. Smith III, K. Y. Lee, J. A. Brum, C. M. Knoedler, J. M. Hong, and D. P. Kern, Phys. Rev. Lett. **62**, 2168 (1989).
[3] T. Demel, D. Heitmann, P. Grambow, and K. Ploog, Phys. Rev. Lett. **64**, 788 (1990).
[4] A. Lorke, J. P. Kotthaus, and K. Ploog, Phys. Rev. Lett. **64**, 2559 (1990).
[5] P. L. McEuen, E. B. Foxman, U. Meirav, M. A. Kastner, Y. Meir, and Ned S. Wingreen, Phys. Rev. Lett. **66**, 1926 (1991).
[6] R. C. Ashoori, H. L. Stormer, J. S. Weiner, L. N. Pfeiffer, K. W. Baldwin, and K. W. West, Phys. Rev. Lett. **71**, 613 (1993).
[7] B. Meurer, D. Heitmann, and K. Ploog, Phys. Rev. Lett. **68**, 1371 (1992).
[8] D. Weiss, M. L. Roukes, A. Menschig, P. Grambow, K. von Klitzing, and G. Weimann, Phys. Rev. Lett. **66**, 2790 (1991).
[9] K. Ensslin and P. Petroff, Phys. Rev. B **41**, 12 307 (1990).
[10] H. Fang and P. J. Stiles, Phys. Rev. B **41**, 10 171 (1990).
[11] A. Lorke, J. P. Kotthaus, and K. Ploog, Phys. Rev. B **44**, 3447 (1991).
[12] G. Berthold, J. Smoliner, V. Rosskopf, E. Gornik, G. Böhm, and G. Weimann, Phys. Rev. B **45**, 11 350 (1992).
[13] G. M. Gusev, Z. D. Kvon, V. M. Kudryashov, L. V. Litvin, Yu. V. Nastaushev, V. T. Dolgopolov, and A. A. Shashkin, Pis'ma Zh. Eksp. Teor. Fiz. **54**, 369 (1991) [JETP Lett. **54**, 364 (1991)].
[14] D. Weiss, K. Richter, A. Menschig, R. Bergmann, H. Schweitzer, K. von Klitzing, and G. Weimann, Phys. Rev. Lett. **70**, 4118 (1993).
[15] K. Kern, D. Heitmann, P. Grambow, Y. Z. Hang, and K. Ploog, Phys. Rev. Lett. **66**, 1618 (1991).
[16] R. Fleischmann, T. Geisel, and K. Ketzmerick, Phys. Rev. Lett. **68**, 1367 (1992).
[17] T. Deruelle, K. Ensslin, P. M. Petroff, A. L. Efros, and F. G. Pikus, Phys. Rev. B **45**, 9082 (1992).
[18] V. G. Burnett, A. L. Efros, and F. G. Pikus, Phys. Rev. B **48**, 14 365 (1993).
[19] C. W. J. Beenakker and H. van Houten, Phys. Rev. Lett. **63**, 1857 (1989).
[20] T. Geisel, R. Ketzmerick, and O. Schedletzky, Phys. Rev. Lett. **69**, 1680 (1992).
[21] R. Fleischmann, T. Geisel, and K. Ketzmerick, Europhys. Lett. **25**, 219 (1994).

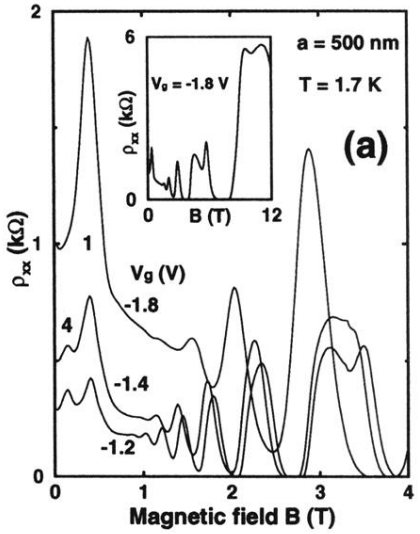

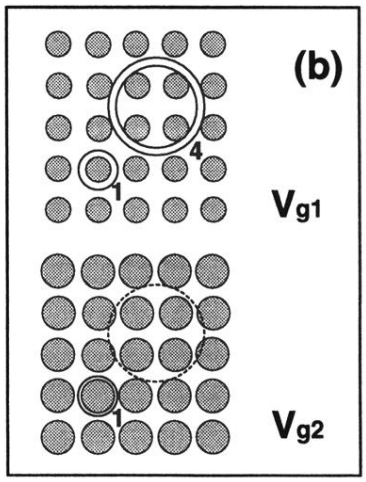

FIG. 1. (a) Magnetoresistance ρ_{xx} for sample 1 with a period of $a = 500$ nm at three different gate voltages V_g as indicated. Commensurability peaks around one and four antidots (labeled 1 and 4) are observed. Peak 4 vanishes at large voltages (large depletion). The inset shows the high-field data at $V_g = -1.8$ V. The temperature is $T = 1.7$ K. (b) Schematic billiard model for different sizes of the depletion zone ($-V_{g2} \geq -V_{g1}$). For strong depletion the motion around four antidots is no longer possible.

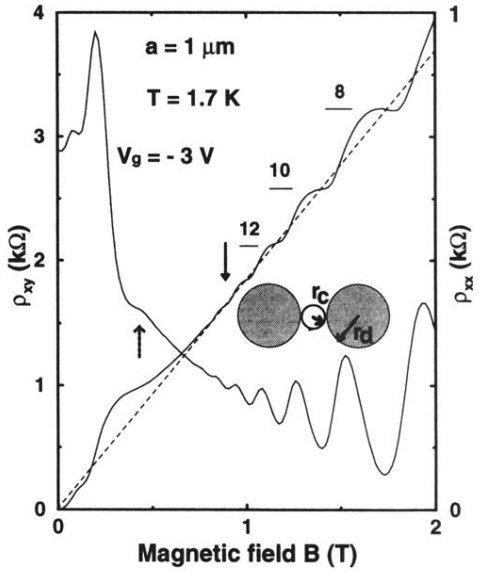

FIG. 3. Magnetoresistance and Hall resistance for sample 2 with a period $a = 1$ μm at $V_g = -3$ V. The solid arrow marks the onset of the observed deviation from which the radius of depletion r_d can be calculated (see inset and text). Weaker structures (marked by a dashed arrow) are associated with interference effects in the potential landscape of the antidots.